Physical Chemistry
Chemical Physics

RSCPublishing

PAPER

Supporting Information

Performance Improvement of Li-Rich Layer-Structured $Li_{1.2}Mn_{0.54}Ni_{0.13}Co_{0.13}O_2$ by Integration with Spinel $LiNi_{0.5}Mn_{1.5}O_4$

Xin Feng, Zhenzhong Yang, Daichun Tang, Qingyu Kong, Lin Gu, Zhaoxiang Wang,* and Liquan Chen

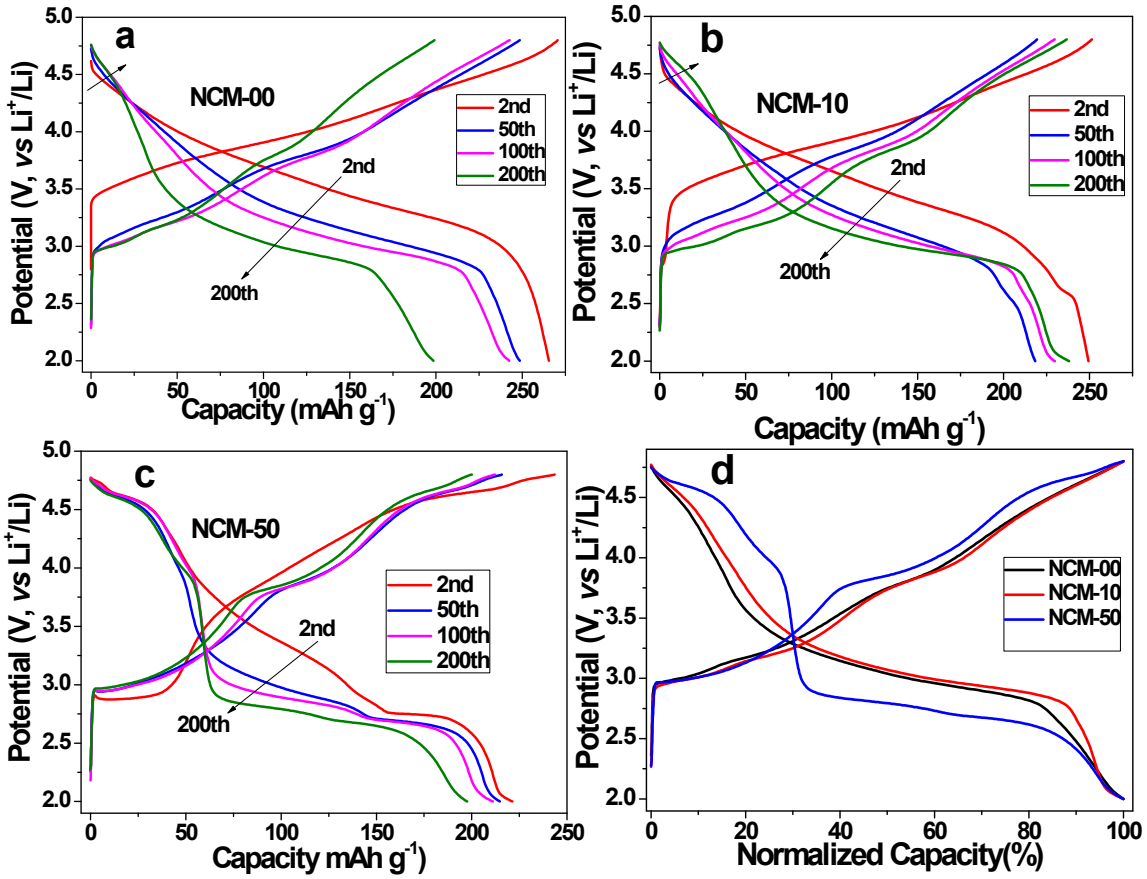

Fig. S1. Voltage profiles of some selected cycles (a-c) and the normalized capacity of the 200th cycle (d) of NCM-00, NCM-10 and NCM-50between 2.0 and 4.8 V *vs*. Li^+/Li at a current density of 60 mA g^{-1}.

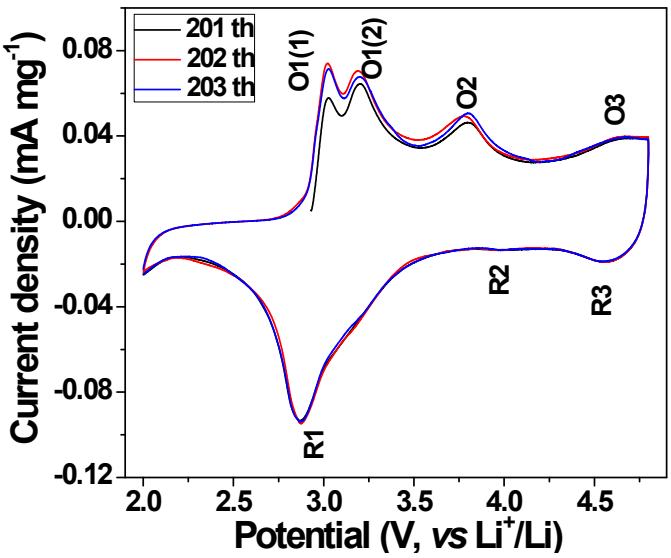

Fig. S2. The cyclic voltammograms of the 201th, 200th and 203rd cycles of NCM-00 electrodes at 0.1 mV s^{-1} between 2.0 and 4.8 V.

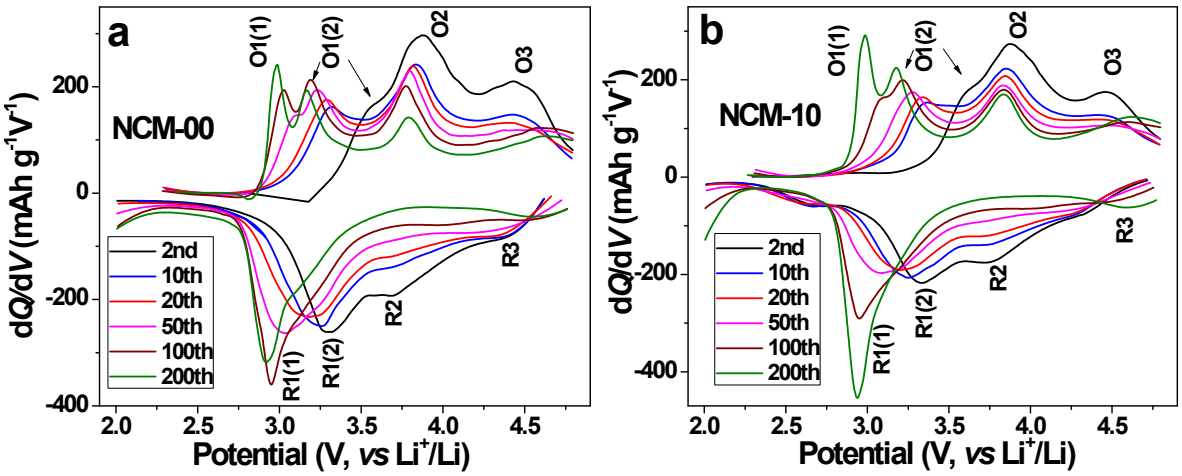

Fig. S3. dQ/dV plots of the 2nd, 10th, 20th, 30th, 50th cycles of NCM-00 (a) and NCM-10 (b) calculated from the data of **Fig. S1**.

In order to observe the variation of each charge/discharge process, the dQ/dV plots of NCM-00 (Fig. S3a) and NCM-10 (Fig. S3b) at different cycles are calculated from the data of Fig. 3, respectively. In the second cycle of NCM-00 (Fig. 3a), there are three distinct processes. The first process about 4.5 V (labeled O3/R3) is attributed to reversible Li^+ extraction/insertion from/into tetrahedral sites. The second process between 3.6 and 3.8 V (labeled O2/R2) can be assigned to the oxidation/reduction of nickel and cobalt ions and the third process in 3.0-3.6 V (labeled O1(2)/R1(2)) mainly contains a cathodic peak corresponding to the oxidation/reduction of Mn ions in the layered phase and MnO_2 derived from Li_2MnO_3.[1] The latter two processes are accompanied with the lithium extraction/insertion from octahedral sites.[2] The intensity of the

O3/R3 and O2/R2 peaks becomes lower, and their positions shift slightly lower upon cycling. However, the peaks of O1(2)/R1(2) process become broader and form a new peak below 3.0 V (marked as O1(1)/R1(1)) attributed to the oxidation/reduction of the Mn ions in the spinel phase,[3,4] additionally, the intensity of the O1(1)/R1(1) peaks are higher than O1(2)/R1(2) peaks in the 200th cycle and the R1(2) peak coincide with the R1(1) peak (R1(1)+ R1(2) peak), suggesting that the layered phase gradually transforms to the spinel phase during cycles, in agreement with previous reports.[2,5] The intensity of the O3 peak reaches a maximum in the 100th cycle, and then somewhat diminishes in the 200th cycle. The dQ/dV plots of NCM-10 are similar to those of NCM-00. However, the intensity of the O2 peak gradually increases after 20 cycles, and the intensities of the O1(2)/R1(2) and O1(1)/R1(1) peaks of NCM-10 continue to increase after 100 cycles until they are higher than that of NCM-00 in the 200th cycle. These differences imply that the layered phase of NCM-10 still remains more electrochemical activation than one of NCM-00 during charge/discharge process after 200 cycles.

The dQ/dV plots and the CV results after 300 cycles indicate that the O1(1) and O1(2) peaks coalesce to form a broad peak (Fig. 4b) of NCM-00 due to the growth of spinel phase and disappearance of the layered phase. However, the O1(1) and O1(2) peaks of NCM-10 (Fig. 3b) shift toward the center after 300 cycles, signifying that layered structure still coexists with spinel structure in NCM-10 after 300 cycles.

Table S1. Cell parameter values of the layered, S1 and S2 phases in the NCM-00 and NCM-10 after 240 cycles

Materials	phases	a (Å)	c (Å)
Cycled NCM-00 or NCM-10	S1 ($Fd\bar{3}m$)	8.062	
	S2 ($Fd\bar{3}m$)	8.228	
	Layered ($R\bar{3}m$)	2.852	14.247
LNMO from JCPDS	Cubic ($Fd\bar{3}m$)	8.173	
NCM-10	Layered ($R\bar{3}m$)	2.850	14.220

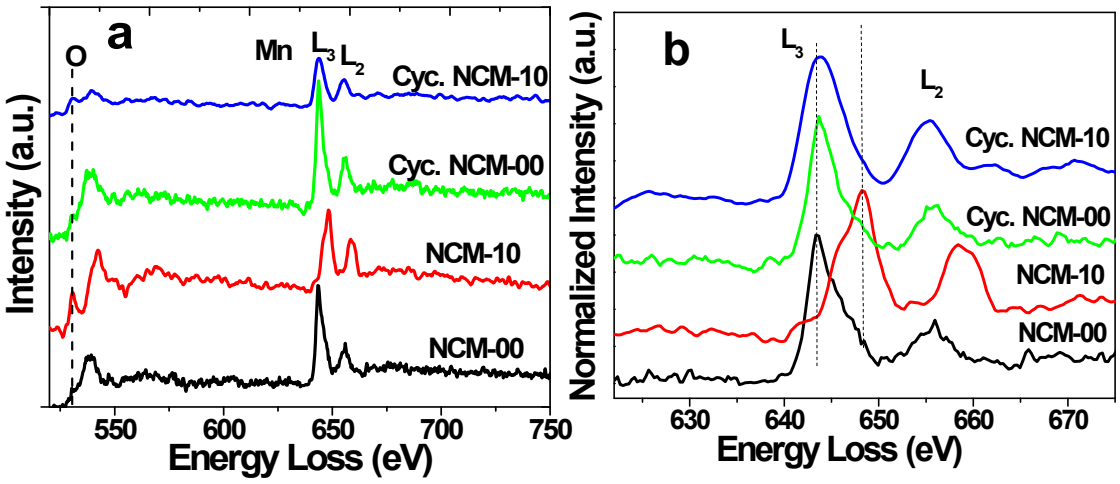

Fig. S4. EELS spectra (a) obtained in the surface of NCM-00 and NCM-10 before and after long-term cycles, and the detail of Mn-L edge in (b).

Electron energy loss spectroscopic (EELS) data are collected from the surface region of particles to confirm the difference of structural changes between NCM-00 and NCM-10 after 240 cycles. Fig. S4 compares the oxygen (O) K-edge and manganese (Mn) L-edge EELS spectra of NCM-00 and NCM-10 before and after 240 cycles at the discharge state. The O prepeaks of different samples were calibrated to the same position for better comparison (Fig. S4a). The O prepeak and O K-edge are caused by hybridization of the unoccupied O 2p orbitals with the transition metal (TM) 3d and 4s or 4p orbitals, respectively.[6,7] As the formation of oxygen vacancies increases the number of the TM 3d electrons, the intensity and position of the O K-edge are sensitive to the average oxidation state of the TM and the content of O vacancies.[8,9] Compared with that of NCM-00, the intensity of O prepeak and the energy of the O K-edge in the NCM-10 increase, probably indicating that the average oxidation state of the TM on the surface becomes higher after integration with spinel LNMO. The intensity of the O prepeak decreases after long-term cycling, suggesting that the average valence state of the TM cations becomes lower.

The variation of the Mn L-edge (Fig. S4b) is consistent with that of the O prepeak and O K-edge. The Mn L-edge of different samples is normalized to L_3-edge for easy comparison. The position of Mn L3-edge of NCM-10 is much higher and the intensity ratio of its L_3- to L_2-edge is larger than in NCM-00. Therefore, the valence of the Mn ions in NCM-10 is higher than in NCM-00. After cycling, the valence of the Mn ions

in the integrated sample decreases, but is still higher than in NCM-00 as is evidenced with the higher energy position of Mn L_3-edge and L_3/L_2 intensity ratio. Decrease of the Mn valence after cycling was previously observed in Li-rich materials,[10,11] as oxygen release from the Li_2MnO_3-like structure in the surface region leads to the reduction of the valence of Mn. The EELS results further confirm that integration with LNMO can impede the release of oxygen from Li_2MnO_3 stabilizes the structure of Li_2MnO_3. In addition, higher oxidation state of Mn in the integrated sample is beneficial for stabilizing the surface structure because formation of soluble Mn^{2+} through the disproportionation reaction at the surface will result in irreversible structural destruction and capacity decay[11,12] as well as increasing the impedance of the anode of a cell. [13]

1 S. H. Kang, C. S. Johnson, J. T. Vaughey, K. Amine and M. M. Thackeray, *J. Electrochem. Soc.* 2006, **153**, A1186.

2 C. S. Johnson, N. C. Li, C. Lefief, J. T. Vaughey and M. M. Thackeray, *Chem. Mater.* 2008, **20**, 6095.

3 D. Mohanty, A. S. Sefat, S. Kalnaus, J. L. Li, R. A. Meisner, E. A. Payzant, D. P. Abraham, D. L. Wood and C. Daniel, *J. Mater. Chem. A* 2013, **1**, 6249.

4 T. Ohzuku, M. Nagayama, K. Tsuji and K. Ariyoshi, *J. Mater. Chem.* 2011, **21**, 10179.

5 B. Song, H. W. Liu, Z. W. Liu, P. F. Xiao, M. O. Lai and L. Lu, *Sci. Rep.* 2013, **3**, 3094.

6 J. H. Rask, B. A. Miner and P. R. Buseck, *Ultramicroscopy* 1987, **21**, 321

7 F. M. F. de Groot, M. Grioni, J. C. Fuggle, J. Ghijsen, G. A. Sawatzky and H. Petersen, *Phys. Rev. B* 1989, **40**, 5715

8 S. Kobayashi, Y. Tokuda, T. Mizoguchi, N. Shibata, Y. Sato, Y. Ikuhara and T. Yamamoto, *J. Appl. Phys.* 2010, **108**, 124903.

9 M. Gu, A. Genc, I. Belharouak, D. P. Wang, K. Amine, S. Thevuthasan, D. R. Baer, J. G. Zhang, N. D. Browning, J. Liu and C. M. Wang, *Chem. Mater.* 2013, **25**, 2319.

10 B. Xu, C. R. Fell, M. Chi and Y. S. Meng, *Energy Environ. Sci.* 2011, **4**, 2223.

11 J. M. Zheng, M. Gu, J. Xiao, P. J. Zuo, C. M. Wang and J. G. Zhang, *Nano Lett.* 2013, **13**, 3824.

12 Y. Xia, Y. Zhou and M. Yoshiot, *J. Electrochem. Soc.* 1997, **144**, 2593

13 C. Zhan, J. Lu, A. J. Kropf, T. Wu, A. N. Jansen, Y. K. Sun, X. Qiu and K. Amine, *Nat. Commun.* 2013, **4**, 2437.